

## Spin-Nernst Effect in Time-Reversal-Invariant Topological Superconductors

Taiki Matsushita<sup>1</sup>, Jiei Ando<sup>1</sup>, Yusuke Masaki<sup>2</sup>, Takeshi Mizushima<sup>1</sup>, Satoshi Fujimoto<sup>1,3</sup> and Ilya Vekhter<sup>4</sup>

<sup>1</sup>Department of Materials Engineering Science, Osaka University, Toyonaka, Osaka 560-8531, Japan

<sup>2</sup>Department of Applied Physics, Graduate School of Engineering, Tohoku University, Sendai, Miyagi 980-8578, Japan

<sup>3</sup>Center for Quantum Information and Quantum Biology, Osaka University, Toyonaka, Osaka 560-8531, Japan

<sup>4</sup>Department of Physics and Astronomy, Louisiana State University, Baton Rouge, Louisiana 70803-4001, USA

 (Received 1 October 2021; accepted 5 February 2022; published 4 March 2022)

We investigate the spin-Nernst effect in time-reversal-invariant topological superconductors, and show that it provides smoking-gun evidence for helical Cooper pairs. The spin-Nernst effect stems from asymmetric, in spin space, scattering of quasiparticles at nonmagnetic impurities, and generates a transverse spin current by the temperature gradient. Both the sign and the magnitude of the effect sensitively depend on the scattering phase shift at impurity sites. Therefore the spin-Nernst effect is uniquely suitable for identifying time-reversal-invariant topological superconducting orders.

DOI: [10.1103/PhysRevLett.128.097001](https://doi.org/10.1103/PhysRevLett.128.097001)

**Introduction.**—In the last decade many researchers investigated topological superconductors (TSCs) with an eye on their application to future technologies such as quantum computation and spintronics [1–7]. These materials are characterized by nontrivial topology of the quasiparticle wave functions, which are responsible for the existence of Majorana quasiparticles [8–10]. The signatures of nontrivial topology appear in transport phenomena, including the quantization of thermal Hall conductivity and tunneling conductance [11–14].

TSCs can be divided into subclasses according to their behavior under time reversal. Condensate in TSCs with spontaneously broken time-reversal symmetry is formed from chiral Cooper pairs with a fixed angular momentum. The key ingredients of time-reversal-invariant (TRI) TSCs are helical Cooper pairs, which are equal mixtures of time-reversed copies of chiral Cooper pairs. If TRI TSCs have an additional discrete symmetry, such as a mirror plane, this symmetry may protect a pair of nodal points in the superconducting gap. In the vicinity of each node, the low-energy Bogoliubov quasiparticles behave as Dirac fermions, and the corresponding class of materials is referred to as Dirac superconductors (DSCs). The  $B$  phase of the superfluid  $^3\text{He}$ , the fully gapped Balian–Werthamer (BW) state, where all three spin components of the triplet order parameter occur in equal measure, is a prototype of TRI TSCs [15–17]. In superconducting materials, there are several candidates for TRI TSCs and DSCs, including  $M_x\text{Bi}_2\text{Se}_3$  ( $M = \text{Cu}, \text{Sr}, \text{Nb}$ ) [18–31],  $\text{U}_{1-x}\text{Th}_x\text{Be}_{13}$  [32–36], and  $\text{Cd}_3\text{As}_2$  [37–39]. Even though a full range of experimental probes has been used for these compounds, including heat capacity, thermal transport, nuclear magnetic resonance, tunneling spectroscopy, and other measurements, the unequivocal “smoking gun” evidence for TSCs and DSCs remains elusive. Hence, it is indispensable

to elucidate physical properties directly associated with helical Cooper pairs.

Among various transport phenomena, the Nernst effect, the transverse electric field generated by a thermal gradient in the presence of a magnetic field, is a powerful tool to capture the symmetry of superconducting order parameters [40]. The Nernst effect induced by flux flow and superconducting fluctuations has been extensively investigated in a variety of materials [41–47]. In  $\text{URu}_2\text{Si}_2$ , the giant Nernst effect observed above the superconducting transition temperature was attributed to the fluctuations of preformed chiral Cooper pairs [48,49]. Thus, the Nernst effect provides a direct probe for Cooper pairs with spontaneously broken time-reversal symmetry.

In this Letter, we show that the *spin Nernst effect* (SNE), the transverse spin current induced by a thermal gradient *without* an applied magnetic field, is a signature of TRI TSCs. On the basis of the quasiclassical transport theory, we demonstrate that in TRI TSCs the impurity scattering of quasiparticles induces the SNE, which reflects the helical nature of the Cooper pairs, schematically shown in Fig. 1.

We reiterate that the SNE in TRI TSCs essentially differs from the conventional Nernst effect due to superconducting

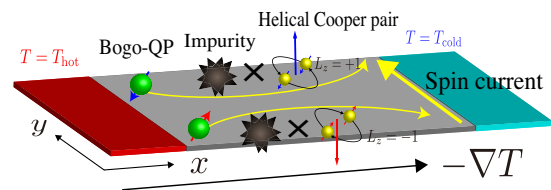


FIG. 1. Schematic image of the SNE in TRI TSCs: spin-dependent asymmetric scattering of the quasiparticles reflecting coupling to different angular momentum components of the Cooper pairs leads to transverse spin current.

fluctuations or vortex motion because (i) a magnetic field is unnecessary, and (ii) the SNE is the bulk transport of homogeneous superconductors below the superconducting transition temperature  $T_c$ . As the SNE arises purely due to the symmetry of Cooper pairs, it provides smoking-gun evidence for helical Cooper pairs in TRI TSCs.

*Quasiclassical Keldysh transport theory.*—The quasiclassical approximation, valid when  $(k_F\xi)^{-1} \ll 1$ , where  $k_F$  is the Fermi momentum and  $\xi$  is the coherence length, is applicable to many superconductors and provides a powerful tool to investigate their transport properties. These are determined from the quasiclassical Green's function  $\check{g}(\epsilon, \mathbf{x}, \mathbf{k}_F)$ , which is an  $8 \times 8$  matrix in the Keldysh and Nambu (particle-hole) space, defined for each  $\mathbf{k}_F$  [50,51]. To leading order in  $(k_F\xi)^{-1}$  the Green's function obeys the quasiclassical Eilenberger equation [52],

$$[\epsilon\check{\tau}_z - \check{\Delta} - \check{\sigma}_{\text{imp}}, \check{g}] + i\mathbf{v}_F \cdot \nabla\check{g} = 0, \quad (1)$$

supplemented by the normalization condition  $\check{g}^2 = -\pi^2$  [50,53]. In Eq. (1),  $\check{\tau}_i$  ( $i = x, y, z$ ) are the Pauli matrices in the Nambu space,  $\mathbf{v}_F$  is the Fermi velocity of normal quasiparticles,  $\check{\sigma}_{\text{imp}}$  is the impurity self-energy, and  $\check{\Delta}$  is the superconducting order parameter matrix, determined from the self-consistency equation [54]. We set  $\hbar = k_B = 1$ , and give the details of other notation and formulation in the Supplemental Material [53].

In the quasiclassical limit, the spin current is obtained from the Keldysh component  $\underline{g}^K$  of the Green's function  $\check{g}$  as

$$\mathbf{J}^{\sigma_\mu} = \frac{1}{2}N(\epsilon_F) \int \frac{d\epsilon}{4\pi i} \langle \text{Tr}[\mathbf{v}_F \underline{\sigma}_\mu \underline{\tau}_z \underline{g}^K] \rangle_{\text{FS}}, \quad (2)$$

where  $N(\epsilon_F)$  is the normal-state density of states at the Fermi energy and  $\underline{\sigma}_\mu$  ( $\mu = x, y, z$ ) is the spin operator in the Nambu space.  $\langle \dots \rangle_{\text{FS}}$  denotes the normalized Fermi surface average. We compute the linear, in the temperature gradient  $(-\nabla T)$ , correction to  $\underline{g}^K$ , accounting for impurity scattering in the self-consistent  $T$ -matrix approximation (SCTA) [55,56]. When implemented in the Keldysh formalism, the anomalous self-energy contains the contribution of the vertex corrections [53]. These vertex corrections are essential for skew scattering [57] and generation of the transverse spin current defined in Eq. (2).

In the following we assume the  $\delta$ -function individual impurity potential with the strength  $V_{\text{imp}}$  and the density of impurities  $n_{\text{imp}}$ . SCTA gives for the impurity self-energy

$$\check{\sigma}_{\text{imp}}(\epsilon) = -\Gamma_{\text{imp}} \left( \cot \delta + \left\langle \frac{\check{g}}{\pi} \right\rangle_{\text{FS}} \right)^{-1}. \quad (3)$$

Here, we defined the normal-state scattering rate  $\Gamma_{\text{imp}} = \{n_{\text{imp}}/[\pi N(\epsilon_F)]\}$  and the scattering phase shift  $\cot \delta = -1/[\pi N(\epsilon_F)V_{\text{imp}}]$ . The limit  $\delta \rightarrow 0$  ( $\delta \rightarrow \pi/2$ )

corresponds to the Born (unitarity) scattering. We then compute the tensor of spin-Nernst coefficients (SNCs),  $\alpha_{jl}^{\sigma_\mu}$ , from the linear response to the thermal gradient,

$$\mathbf{J}_j^{\sigma_\mu} = \alpha_{jl}^{\sigma_\mu} (-\partial_l T). \quad (4)$$

This expression neglects a possible normal-state spin-Nernst coefficient due to spin-orbit interaction, but this contribution is expected to be very small for  $T_c \ll E_{\text{SO}}$ , where  $E_{\text{SO}} \sim 10^3$  K is the characteristic spin-orbital energy scale [58,59].

*SNE in DSCs.*—As a prototype of TRI TSCs, we consider the three-dimensional helical  $p$ -wave superconducting gap on the spherical Fermi surface, where the  $d$  vector is given by

$$\mathbf{d}_{\text{DSC},xy}(\mathbf{k}) = \frac{\Delta}{k_F} (k_x, k_y, 0). \quad (5)$$

This is an example of a DSC since the gap has two Dirac points at the south and north poles on the Fermi sphere. This simple gap structure enables one to capture essence of the SNE in TRI TSCs. The same model describes the low-energy physics of DSCs in  $\text{Cd}_3\text{As}_2$ , and the results below are directly applicable to this material [39]. The spin projection  $\sigma_z$  is a good quantum number for Eq. (5), and the quasiparticle states are block diagonal in terms of  $\sigma_z = \pm 1$ . The Cooper pairs in the  $\sigma_z = +1$  ( $\sigma_z = -1$ ) sector condense into the  $L_z = -1$  ( $L_z = +1$ ) eigenstates of the angular momentum  $k_x - ik_y$  ( $k_x + ik_y$ ). Each sector is chiral and breaks time reversal and mirror symmetries. These broken symmetries give rise to the asymmetric quasiparticle scattering at impurities, which induces a transverse flow of quasiparticles along the direction determined by the sign of chirality [60–63]. Since the helical pairing state or DSCs can be regarded as the superposition of chiral Cooper pairs with opposite chiralities in different spin sectors, asymmetric scattering on nonmagnetic impurities becomes spin selective and thus generates the transverse spin current (Fig. 1).

Motivated by this, we consider the spin-Nernst signal for the temperature gradient along the  $y$  direction. Figure 2(a) shows the temperature dependence of the spin-Nernst coefficient for different impurity scattering phase shifts. The SNC is sensitive to the scattering phase shift. Both the low-temperature slope and the maximum value below  $T_c$  increase as the phase shift approaches the unitarity limit,  $\delta \rightarrow \pi/2$ . Remarkably, the sign of the SNC changes as a function of  $\delta$ .

This evolution can be understood from the low-temperature expansion of  $\underline{g}^K$  in Eq. (2) [55]. Since the nonequilibrium Keldysh Green's function is proportional to  $\text{sech}^2(\epsilon/2T)$ , it entails a frequency cutoff  $\epsilon \sim T$  that serves as a small parameter at low  $T$ . We find for the SNC in clean DSCs as  $T \rightarrow 0$  [53],

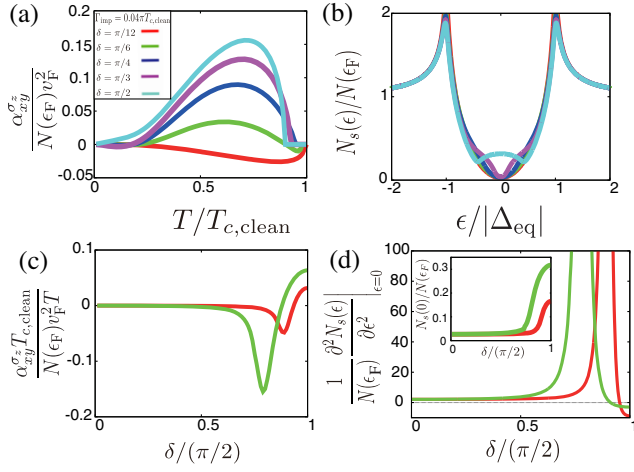


FIG. 2. (a) Temperature dependences of the SNC ( $\alpha_{xy}^{\sigma_z}$ ) and (b) quasiparticle DOS in DSCs at  $T = 0.01\pi T_{c,\text{clean}}$  with a critical temperature at the clean limit  $T_{c,\text{clean}}$ . For panels (a),(b), we set the impurity scattering rate  $\Gamma_{\text{imp}} = 0.04\pi T_{c,\text{clean}}$ , and the scattering phase shift  $\delta = (\pi/12)$  (red),  $\pi/6$  (green),  $\pi/4$  (blue),  $\pi/3$  (purple), and  $\pi/2$  (light blue). (c) The scattering phase-shift dependence of  $\alpha_{xy}^{\sigma_z}$  in DSCs at  $T = 0.01T_{c,\text{clean}}$  and (d) the second-order derivative of the DOS with respect to  $\epsilon$ . For panels (c),(d), we set the impurity scattering rate  $\Gamma_{\text{imp}} = 0.01\pi T_{c,\text{clean}}$  for the red curves, and  $\Gamma_{\text{imp}} = 0.04\pi T_{c,\text{clean}}$  for the green curves, respectively. The inset in panel (d) shows the phase-shift dependence of the residual DOS  $N_s(0)$ .

$$\frac{\alpha_{xy}^{\sigma_z}}{N(\epsilon_F)v_F^2} = -\frac{\pi^2\gamma\Gamma_{\text{imp}}T}{12} \frac{\cot^2\delta - n_s^2}{(\cot^2\delta + n_s^2)^2} \times \left\langle \frac{|\mathbf{d}_{\text{eq}}(\mathbf{k}_F)|^2}{[|\mathbf{d}_{\text{eq}}(\mathbf{k}_F)|^2 + \gamma^2]^{3/2}} \right\rangle_{\text{FS}} + \mathcal{O}(T^2, \Gamma_{\text{imp}}^3). \quad (6)$$

The complete expression of the SNC, including higher-order terms for  $\Gamma_{\text{imp}}$ , is given in the Supplemental Material [53]. In Eq. (6), we introduced the residual quasiparticle DOS at the Fermi energy in the superconducting state,  $n_s = N_s(0)/N(\epsilon_F) = -(1/4\pi)\langle \text{Tr} \text{Im}[\tau_z g_{\text{eq}}^R(0)] \rangle_{\text{FS}}$ , and the impurity self-energy at equilibrium,  $\gamma \equiv (i/4)\text{Tr}[\underline{\tau}_z \underline{\sigma}_{\text{imp,eq}}^R(0)]$ . It is seen from Fig. 2(b) that as the phase shift approaches the unitarity limit, the spectral weight around the coherence peaks  $\epsilon \approx \pm|\Delta_{\text{eq}}|$  reduces, while  $N_s(0)$  increases. The transfer of the spectral weight in the DOS reflects the formation of the impurity bands; see discussion below.

It is clear from Eq. (6) that, in agreement with Fig. 2(a), the SNC changes the sign as a function of the scattering phase shift from negative at weak scattering,  $\cot\delta \gg 1$ , to positive near unitarity,  $\cot\delta \rightarrow 0$ . This behavior is shown in Fig. 2(c), where the critical phase shift is  $\delta_c \simeq 0.94 \times (\pi/2)$  for  $\Gamma_{\text{imp}} = 0.01\pi T_{c,\text{clean}}$ , and  $\delta_c \simeq 0.88 \times (\pi/2)$  for  $\Gamma_{\text{imp}} = 0.04\pi T_{c,\text{clean}}$ . Expansion in the phase shift at low energies near the unitarity limit gives the sign change occurring at

$\delta_c = (\pi/2)(1 - \chi_c)$  with  $\chi_c \approx \sqrt{\Gamma_{\text{imp}}/\pi\Delta_{\text{eq}}(T=0)}$  in qualitative agreement with the numerical results.

Another striking feature in Fig. 2(c) is a large peak in SNC at the intermediate phase shift. Recall that the transverse transport coefficients reflect the asymmetry of scattering convoluted with the variation of the density of states near the Fermi surface [64]. In unconventional superconductors, the impurity potential gives rise to the impurity quasibound (resonant) states, whose position shifts from the gap edge to midgap as the phase shift approaches the unitarity limit [see Fig. 2(b)]. For finite impurity concentrations, these states (symmetrically positioned at the electron- and hole-sides of the spectrum) broaden into the impurity bands. Sizeable DOS at the Fermi level first appears when the impurity band touches the Fermi energy. At that point the strong variation of the DOS with the energy amplifies the scattering asymmetry near the Fermi energy. A quantitative measure of when this happens is the band curvature at the origin,  $(d^2N_s/d\epsilon^2)|_{\epsilon=0}$ , which is maximal when the bands first reach  $\epsilon = 0$ . The corresponding phase shift is estimated to be  $\delta = (\pi/2)(1 - 2\chi_c)$ . As shown in Figs. 2(c) and 2(d), the peak in the band curvature coincides with the peak in SNC in Fig. 2(c).

Since the mechanism for the SNE described here relies on the structure of the emergent impurity-induced bands, the same picture should be applicable to fully gapped TRI TSCs, which are considered below.

*The BW state in disordered media.*—A well-studied example of fully gapped TRI TSCs is the BW state,  $\mathbf{d}_{\text{BW}}(\mathbf{k}) = (\Delta/k_F)(k_x, k_y, k_z)$ , realized in the *B* phase of the superfluid  $^3\text{He}$  [15,16]. Here we consider the BW state in the presence of nonmagnetic impurities. At the qualitative level, the SNE in the BW state shares its origin with that in DSCs discussed above. The BW state can be viewed as the superposition of three helical *p*-wave pairing channels,

$$\mathbf{d}_{\text{BW}} = \frac{1}{2}(\mathbf{d}_{\text{DSC},xy} + \mathbf{d}_{\text{DSC},yz} + \mathbf{d}_{\text{DSC},zx}), \quad (7)$$

with  $\mathbf{d}_{\text{DSC},xy}(\mathbf{k}) = (\Delta/k_F)(k_x, k_y, 0)$ ,  $\mathbf{d}_{\text{DSC},zx}(\mathbf{k}) = (\Delta/k_F)(k_x, 0, k_z)$ , and  $\mathbf{d}_{\text{DSC},yz}(\mathbf{k}) = (\Delta/k_F)(0, k_y, k_z)$ . Figure 3 shows the temperature dependences of the SNC for several phase shifts, which are qualitatively same as those in DSCs discussed above.

The spin structure of these components gives rise to the SNE similar to the case of DSCs, with the result shown in Fig. 3(a). The SO(3) symmetry preserved in the BW state dictates the relations between the tensor elements of the SNC,

$$\alpha_{xy}^{\sigma_z} = \alpha_{yz}^{\sigma_x} = \alpha_{zx}^{\sigma_y} = -\alpha_{yx}^{\sigma_z} = -\alpha_{zy}^{\sigma_x} = -\alpha_{xz}^{\sigma_y}. \quad (8)$$

These relations are also maintained by the  $A_u$  irreducible representation of the  $O_h$  crystals. Equation (8) can be

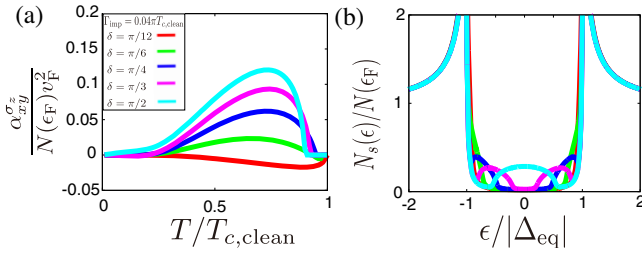


FIG. 3. (a) The temperature dependences of the SNC and (b) the DOS in the dirty BW state at  $T = 0.01T_{c,\text{clean}}$ . We set the impurity scattering rate  $\Gamma_{\text{imp}} = 0.04\pi T_{c,\text{clean}}$  and the phase shift  $\delta = (\pi/12), (\pi/6), (\pi/4), (\pi/3), (\pi/2)$ . The unitarity limit  $\delta \rightarrow \pi/2$  describes the gapless BW state.

understood from Eq. (7): When the temperature gradient is applied along the  $y$  direction,  $\mathbf{d}_{\text{DSC},xy}$  ( $\mathbf{d}_{\text{DSC},yz}$ ) pairing gives rise to the spin current  $\mathbf{J}^{\sigma_z}$  ( $\mathbf{J}^{\sigma_x}$ ) along the  $x$  direction ( $z$  direction).

As in DSCs, the quasiparticle DOS in the BW state with nonmagnetic impurities has impurity bound states, where the spectral weight is transferred from the coherence peaks around  $\epsilon \approx \pm\Delta$  to the lower energies [Fig. 3(b)]. The width of the band formed around these resonance energies depends on the phase shift of the scattering as well as the impurity concentration. When the impurity bands reach  $\epsilon = 0$ , the system realizes the “gapless” BW state. Even though the BW state in the clean limit is fully gapped, the quasiparticles of the impurity bound states are responsible for the SNE. Notably, in  $\delta \rightarrow \pi/2$ , the SNCs show the  $T$ -linear behavior at the low temperature, which we attribute to the finite impurity-induced DOS at the Fermi level [see Figs. 3(a) and 3(b)].

*Application to candidate materials.*—A well-established example of gapped TRI TSCs is the  $B$  phase of superfluid  ${}^3\text{He}$ . For  ${}^3\text{He}$ , strong (near-unitarity) impurity scattering can be engineered by highly porous silica aerogel [65–67], realizing the “dirty” BW state [68–71]. The aerogel is composed of silica strands (diameter 30 Å), separated by the mean distance that is comparable to or less than the superfluid coherence length. The spin flip scattering by magnetic surface solid is suppressed by coating aerogel with a few layers of  ${}^4\text{He}$  atoms [72]. Hence, the properties of the liquid  ${}^3\text{He}$  in the aerogel are well described by the homogeneous scattering model [68], where the aerogel is represented by randomly distributed nonmagnetic scattering centers. The model has two parameters: the phase shift  $\delta$  and the mean free path  $\ell$  determined by the aerogel geometry. Several experiments identified the “gapless” BW state over the pressure range  $p = 6\text{--}34$  bar [73–76], which is in good agreement with the homogeneous scattering model with  $\delta \rightarrow \pi/2$  and  $\ell \approx 1800$  Å for 98% porosity [68–70]. Then the normal-state scattering rate for the aerogel is estimated as  $\Gamma_{\text{imp}} = \hbar v_F / (2\ell \sin^2 \delta) \approx$

$0.1\text{--}0.2\pi T_{c,\text{clean}}$ . We find the qualitatively same behavior of the SNC as that in Fig. 3(a) even for such large  $\Gamma_{\text{imp}}$ . Hence, the spin-Nernst effect can be utilized as a thermal generation of quasiparticle-mediated spin current in superfluid  ${}^3\text{He}$ .

Another interesting example is the heavy-fermion superconductor  $\text{U}_{1-x}\text{Th}_x\text{Be}_{13}$ , discovered in the 1980s [77]. It is a spin-triplet superconductor with three distinct superconducting phases in the  $x\text{--}T$  plane. At  $x = 0$ , the “parent” material  $\text{UBe}_{13}$  undergoes superconducting phase transition at  $T_{2c}(x = 0) \sim 0.85$  K. For  $0 \leq x < 0.02$ , the critical temperature  $T_{2c}(x)$  decreases with increasing Th concentration,  $x$ . This superconducting phase is referred to as the  $C$  phase. In a narrow dopant region  $0.02 \leq x \leq 0.04$ , an additional superconducting transition occurs at  $T_{1c}(x) \geq T_{2c}(x)$ , and the time-reversal symmetry is spontaneously broken below  $T_{2c}(x)$  [78–80]. The superconducting phase in  $T_{2c}(x) \leq T \leq T_{1c}(x)$  is referred to as the  $A$ , phase and the time-reversal symmetry broken phase is called the  $B$  phase [34,36].

In spite of many efforts, the pairing symmetry of this material remains unresolved. One possible scenario is an accidental degeneracy of the order parameters belonging to different irreducible representations of the  $O_h$  group [35]. Another possibility is the realization of the odd-parity  $E_u$  state [33]. Both scenarios predict DSCs in the  $A$  phase and TRI TSCs in the  $C$  phase.

However, the onset of the  $E_u$  state is accompanied by a nematic phase transition with broken rotational symmetry, leading to a different type of helical Cooper pairing from the accidental scenario [32]. The Dirac superconducting  $A$  phase supported by the accidental scenario manifests a finite SNC  $\alpha_{xy}^{\sigma_z}$ ,  $\alpha_{yz}^{\sigma_x}$ , and  $\alpha_{zx}^{\sigma_y}$ , whereas only  $\alpha_{xy}^{\sigma_z}$  is finite in the  $E_u$  state. For the TRI TSC  $C$  phase, the nematicity in the  $E_u$  state leads to the anisotropy of the SNC, while there is no anisotropy of the SNC in the same phase within the accidental scenario. Thus, measurements of the SNE presented in this paper provide smoking-gun evidence for identifying the superconducting symmetry in  $\text{U}_{1-x}\text{Th}_x\text{Be}_{13}$  and other complex materials.

We note that in the weak coupling limit the form of the gap function fully determines the topological properties of the superconducting state (for a given Fermi surface). Therefore our results remain valid for systems where the parity of the superconducting state is determined, in real space, by orbital mixing, such as  $\text{Cd}_3\text{As}_2$  and doped  $\text{Bi}_2\text{Se}_3$ . In the momentum space these order parameters map on the examples considered above [28,37].

*Conclusion.*—We established that the SNE provides direct evidence for helical Cooper pairs in TRI TSCs. The origin of this SNE is the spin-dependent scattering of quasiparticles through the helical Cooper pairs on nonmagnetic impurities. The SNE has strong dependence on the scattering phase shift, and changes the sign of the SNC

on approaching the unitarity limit. The SNE is detectable in the TSC candidate materials, and its experimental verification is feasible.

We finally comment on an interesting future study. In this letter, we focused on the SNE in bulk, but the SNE is also possible in the surfaces. In the surfaces of the TRI TSCs, the low-energy quasiparticles behave as helical fermions and carry the circulating spin current [81]. The SNE at the surfaces is expected through helical fermions or the parity mixing of the order parameters [82].

T. Matsushita is grateful to A. Daido, A. Shitade, and Y. Yanase for useful discussions. Discussion with A. Daido for TRI TSC is one of the motivations for this research. T. Matsushita was supported by a Japan Society for the Promotion of Science (JSPS) Fellowship for Young Scientists and by JSPS KAKENHI Grant No. JP19J20144, and Y.M. was supported in part by the JSPS Early-Career Scientists Grant No. JP19K14662. I. V. was supported in part by NSF Grant No. DMR-1410741. This work was initiated at Louisiana State University, and also supported by JST CREST Grant No. JPMJCR19T5, Japan, and the Grant-in-Aid for Scientific Research on Innovative Areas “Quantum Liquid Crystals (JP20H05163)” from JSPS of Japan, and JSPS KAKENHI (Grants No. JP17K05517, No. JP20K03860, No. JP20H01857, and No. JP21H01039).

- 
- [1] A. Y. Kitaev, Unpaired Majorana fermions in quantum wires, *Phys. Usp.* **44**, 131 (2001).
- [2] X.-L. Qi and S.-C. Zhang, Topological insulators and superconductors, *Rev. Mod. Phys.* **83**, 1057 (2011).
- [3] L. Fu and C. L. Kane, Superconducting Proximity Effect and Majorana Fermions at the Surface of a Topological Insulator, *Phys. Rev. Lett.* **100**, 096407 (2008).
- [4] J. Linder and J. W. Robinson, Superconducting spintronics, *Nat. Phys.* **11**, 307 (2015).
- [5] T. Wakamura, H. Akaike, Y. Otori, Y. Niimi, S. Takahashi, A. Fujimaki, S. Maekawa, and Y. Otani, Quasiparticle-mediated spin Hall effect in a superconductor, *Nat. Mater.* **14**, 675 (2015).
- [6] T. Wakamura, N. Hasegawa, K. Ohnishi, Y. Niimi, and Y. C. Otani, Spin Injection into a Superconductor with Strong Spin-Orbit Coupling, *Phys. Rev. Lett.* **112**, 036602 (2014).
- [7] R. Ghadimi, M. Kargarian, and S. A. Jafari, Gap-filling states induced by disorder and Zeeman coupling in the nodeless chiral superconducting Bi/Ni bilayer system, *Phys. Rev. B* **100**, 024502 (2019).
- [8] J. Alicea, New directions in the pursuit of Majorana fermions in solid state systems, *Rep. Prog. Phys.* **75**, 076501 (2012).
- [9] M. Sato and S. Fujimoto, Majorana fermions and topology in superconductors, *J. Phys. Soc. Jpn.* **85**, 072001 (2016).
- [10] M. Sato and Y. Ando, Topological superconductors: A review, *Rep. Prog. Phys.* **80**, 076501 (2017).
- [11] N. Read and D. Green, Paired states of fermions in two dimensions with breaking of parity and time-reversal symmetries and the fractional quantum Hall effect, *Phys. Rev. B* **61**, 10267 (2000).
- [12] K. Nomura, S. Ryu, A. Furusaki, and N. Nagaosa, Cross-Correlated Responses of Topological Superconductors and Superfluids, *Phys. Rev. Lett.* **108**, 026802 (2012).
- [13] H. Sumiyoshi and S. Fujimoto, Quantum thermal Hall effect in a time-reversal-symmetry-broken topological superconductor in two dimensions: Approach from bulk calculations, *J. Phys. Soc. Jpn.* **82**, 023602 (2013).
- [14] K. T. Law, P. A. Lee, and T. K. Ng, Majorana Fermion Induced Resonant Andreev Reflection, *Phys. Rev. Lett.* **103**, 237001 (2009).
- [15] A. J. Leggett, A theoretical description of the new phases of liquid He3, *Rev. Mod. Phys.* **47**, 331 (1975).
- [16] T. Mizushima, Y. Tsutsumi, T. Kawakami, M. Sato, M. Ichioka, and K. Machida, Symmetry-protected topological superfluids and superconductors—from the basics to  $^3\text{He}$ —, *J. Phys. Soc. Jpn.* **85**, 022001 (2016).
- [17] G. E. Volovic, *The universe in a helium droplet* (Oxford, New York, 2003).
- [18] L. A. Wray, S.-Y. Xu, Y. Xia, Y. San Hor, D. Qian, A. V. Fedorov, H. Lin, A. Bansil, R. J. Cava, and M. Z. Hasan, Observation of topological order in a superconducting doped topological insulator, *Nat. Phys.* **6**, 855 (2010).
- [19] M. Kriener, K. Segawa, Z. Ren, S. Sasaki, S. Wada, S. Kuwabata, and Y. Ando, Electrochemical synthesis and superconducting phase diagram of  $\text{Cu}_x\text{Bi}_2\text{Se}_3$ , *Phys. Rev. B* **84**, 054513 (2011).
- [20] M. Kriener, K. Segawa, Z. Ren, S. Sasaki, and Y. Ando, Bulk Superconducting Phase with a Full Energy Gap in the Doped Topological Insulator  $\text{Cu}_x\text{Bi}_2\text{Se}_3$ , *Phys. Rev. Lett.* **106**, 127004 (2011).
- [21] K. Matano, M. Kriener, K. Segawa, Y. Ando, and G.-q. Zheng, Spin-rotation symmetry breaking in the superconducting state of  $\text{Cu}_x\text{Bi}_2\text{Se}_3$ , *Nat. Phys.* **12**, 852 (2016).
- [22] L. Fu and E. Berg, Odd-Parity Topological Superconductors: Theory and Application to  $\text{Cu}_x\text{Bi}_2\text{Se}_3$ , *Phys. Rev. Lett.* **105**, 097001 (2010).
- [23] Y. S. Hor, A. J. Williams, J. G. Checkelsky, P. Roushan, J. Seo, Q. Xu, H. W. Zandbergen, A. Yazdani, N. P. Ong, and R. J. Cava, Superconductivity in  $\text{Cu}_x\text{Bi}_2\text{Se}_3$  and its Implications for Pairing in the Undoped Topological Insulator, *Phys. Rev. Lett.* **104**, 057001 (2010).
- [24] S. Sasaki, M. Kriener, K. Segawa, K. Yada, Y. Tanaka, M. Sato, and Y. Ando, Topological Superconductivity in  $\text{Cu}_x\text{Bi}_2\text{Se}_3$ , *Phys. Rev. Lett.* **107**, 217001 (2011).
- [25] S. Yonezawa, K. Tajiri, S. Nakata, Y. Nagai, Z. Wang, K. Segawa, Y. Ando, and Y. Maeno, Thermodynamic evidence for nematic superconductivity in  $\text{Cu}_x\text{Bi}_2\text{Se}_3$ , *Nat. Phys.* **13**, 123 (2017).
- [26] S. Sasaki and T. Mizushima, Superconducting doped topological materials, *Physica (Amsterdam)* **514C**, 206 (2015).
- [27] S. Yonezawa, Bulk topological superconductors, *AAPPS Bull.* **26**, 3 (2016).
- [28] S. Yonezawa, Nematic superconductivity in doped  $\text{Bi}_2\text{Se}_3$  topological superconductors, *Condens. Matter* **4**, 2 (2019).
- [29] H. Uematsu, T. Mizushima, A. Tsuruta, S. Fujimoto, and J. A. Sauls, Chiral Higgs Mode in Nematic Superconductors, *Phys. Rev. Lett.* **123**, 237001 (2019).

- [30] Y. Pan, A. Nikitin, G. Araizi, Y. Huang, Y. Matsushita, T. Naka, and A. De Visser, Rotational symmetry breaking in the topological superconductor  $\text{Sr}_x\text{Bi}_2\text{Se}_3$  probed by upper-critical field experiments, *Sci. Rep.* **6**, 1 (2016).
- [31] A. M. Nikitin, Y. Pan, Y. K. Huang, T. Naka, and A. de Visser, High-pressure study of the basal-plane anisotropy of the upper critical field of the topological superconductor  $\text{Sr}_x\text{Bi}_2\text{Se}_3$ , *Phys. Rev. B* **94**, 144516 (2016).
- [32] K. Machida, Spin triplet nematic pairing symmetry and superconducting double transition in  $\text{U}_{1-x}\text{Th}_x\text{Be}_{13}$ , *J. Phys. Soc. Jpn.* **87**, 033703 (2018).
- [33] T. Mizushima and M. Nitta, Topology and symmetry of surface Majorana arcs in cyclic superconductors, *Phys. Rev. B* **97**, 024506 (2018).
- [34] Y. Shimizu, S. Kittaka, S. Nakamura, T. Sakakibara, D. Aoki, Y. Homma, A. Nakamura, and K. Machida, Quasiparticle excitations and evidence for superconducting double transitions in monocrystalline  $\text{U}_{0.97}\text{Th}_{0.03}\text{Be}_{13}$ , *Phys. Rev. B* **96**, 100505(R) (2017).
- [35] M. Sigrist and T. M. Rice, Phenomenological theory of the superconductivity phase diagram of  $\text{U}_{1-x}\text{Th}_x\text{Be}_{13}$ , *Phys. Rev. B* **39**, 2200 (1989).
- [36] R. H. Heffner, J. L. Smith, J. O. Willis, P. Birrer, C. Baines, F. N. Gyax, B. Hitti, E. Lippelt, H. R. Ott, A. Schenck, E. A. Knetsch, J. A. Mydosh, and D. E. MacLaughlin, New Phase Diagram for  $(\text{U}, \text{Th})\text{Be}_{13}$ : A Muon-Spin-Resonance and  $\text{H}_{\text{C1}}$  Study, *Phys. Rev. Lett.* **65**, 2816 (1990).
- [37] T. Hashimoto, S. Kobayashi, Y. Tanaka, and M. Sato, Superconductivity in doped Dirac semimetals, *Phys. Rev. B* **94**, 014510 (2016).
- [38] S. Kobayashi and M. Sato, Topological Superconductivity in Dirac Semimetals, *Phys. Rev. Lett.* **115**, 187001 (2015).
- [39] T. Matsushita, T. Liu, T. Mizushima, and S. Fujimoto, Charge/spin supercurrent and the Fulde-Ferrell state induced by crystal deformation in Weyl/Dirac superconductors, *Phys. Rev. B* **97**, 134519 (2018).
- [40] K. Behnia and H. Aubin, Nernst effect in metals and superconductors: A review of concepts and experiments, *Rep. Prog. Phys.* **79**, 046502 (2016).
- [41] M. Zeh, H.-C. Ri, F. Kober, R. P. Huebener, A. V. Ustinov, J. Mannhart, R. Gross, and A. Gupta, Nernst Effect in Superconducting Y-Ba-Cu-O, *Phys. Rev. Lett.* **64**, 3195 (1990).
- [42] Y. Wang, L. Li, and N. P. Ong, Nernst effect in high- $T_c$  superconductors, *Phys. Rev. B* **73**, 024510 (2006).
- [43] I. Ussishkin, S. L. Sondhi, and D. A. Huse, Gaussian Superconducting Fluctuations, Thermal Transport, and the Nernst Effect, *Phys. Rev. Lett.* **89**, 287001 (2002).
- [44] I. Ussishkin, Superconducting fluctuations and the Nernst effect: A diagrammatic approach, *Phys. Rev. B* **68**, 024517 (2003).
- [45] H. Kontani, Nernst Coefficient and Magnetoresistance in High- $T_c$  Superconductors: The Role of Superconducting Fluctuations, *Phys. Rev. Lett.* **89**, 237003 (2002).
- [46] A. Pourret, H. Aubin, J. Lesueur, C. Marrache-Kikuchi, L. Berge, L. Dumoulin, and K. Behnia, Observation of the Nernst signal generated by fluctuating Cooper pairs, *Nat. Phys.* **2**, 683 (2006).
- [47] C. Zhang, S. Tewari, V. M. Yakovenko, and S. Das Sarma, Anomalous Nernst effect from a chiral d-density-wave state in underdoped cuprate superconductors, *Phys. Rev. B* **78**, 174508 (2008).
- [48] H. Sumiyoshi and S. Fujimoto, Giant Nernst and Hall effects due to chiral superconducting fluctuations, *Phys. Rev. B* **90**, 184518 (2014).
- [49] T. Yamashita, Y. Shimoyama, Y. Haga, T. Matsuda, E. Yamamoto, Y. Onuki, H. Sumiyoshi, S. Fujimoto, A. Levchenko, T. Shibauchi *et al.*, Colossal thermomagnetic response in the exotic superconductor  $\text{URu}_2\text{Si}_2$ , *Nat. Phys.* **11**, 17 (2015).
- [50] G. Eilenberger, Transformation of Gorkov's equation for type II superconductors into transport-like equations, *Z. Phys. A* **214**, 195 (1968).
- [51] J. W. Serene and D. Rainer, The quasiclassical approach to superfluid  $^3\text{He}$ , *Phys. Rep.* **101**, 221 (1983).
- [52] T. Kobayashi, T. Matsushita, T. Mizushima, A. Tsuruta, and S. Fujimoto, Negative Thermal Magnetoresistivity as a Signature of a Chiral Anomaly in Weyl Superconductors, *Phys. Rev. Lett.* **121**, 207002 (2018).
- [53] See Supplemental Material at <http://link.aps.org/supplemental/10.1103/PhysRevLett.128.097001> for quasiclassical Keldysh theory.
- [54] M. Sigrist and K. Ueda, Phenomenological theory of unconventional superconductivity, *Rev. Mod. Phys.* **63**, 239 (1991).
- [55] M. J. Graf, S. K. Yip, J. A. Sauls, and D. Rainer, Electronic thermal conductivity and the Wiedemann-Franz law for unconventional superconductors, *Phys. Rev. B* **53**, 15147 (1996).
- [56] A. Vorontsov and I. Vekhter, Unconventional superconductors under a rotating magnetic field. II. Thermal transport, *Phys. Rev. B* **75**, 224502 (2007).
- [57] N. Nagaosa, J. Sinova, S. Onoda, A. H. MacDonald, and N. P. Ong, Anomalous hall effect, *Rev. Mod. Phys.* **82**, 1539 (2010).
- [58] A. B. Vorontsov, I. Vekhter, and M. Eschrig, Surface Bound States and Spin Currents in Noncentrosymmetric Superconductors, *Phys. Rev. Lett.* **101**, 127003 (2008).
- [59] A. Dyrdał, J. Barnaś, and V. K. Dugaev, Spin Hall and spin Nernst effects in a two-dimensional electron gas with Rashba spin-orbit interaction: Temperature dependence, *Phys. Rev. B* **94**, 035306 (2016).
- [60] S. Yip, Low temperature thermal hall conductivity of a nodal chiral superconductor, *Supercond. Sci. Technol.* **29**, 085006 (2016).
- [61] V. Ngampruetikorn and J. A. Sauls, Impurity-Induced Anomalous Thermal Hall Effect in Chiral Superconductors, *Phys. Rev. Lett.* **124**, 157002 (2020).
- [62] H. Ikegami, Y. Tsutsumi, and K. Kono, Chiral symmetry breaking in superfluid  $^3\text{He-A}$ , *Science* **341**, 59 (2013).
- [63] O. Shevtsov and J. A. Sauls, Electron bubbles and Weyl fermions in chiral superfluid  $^3\text{He-A}$ , *Phys. Rev. B* **94**, 064511 (2016).
- [64] B. Arfi, H. Bahlouli, C. J. Pethick, and D. Pines, Unusual Transport Effects in Anisotropic Superconductors, *Phys. Rev. Lett.* **60**, 2206 (1988).
- [65] W. P. Halperin, H. Choi, J. P. Davis, and J. Pollanen, Impurity effects of aerogel in superfluid  $^3\text{He}$ , *J. Phys. Soc. Jpn.* **77**, 111002 (2008).

- [66] W. P. Halperin, J. M. Parpia, and J. A. Sauls, Superfluid helium-3 in confined quarters, *Phys. Today* **71**, 30 (2018).
- [67] W. Halperin, Superfluid  $^3\text{He}$  in aerogel, *Annu. Rev. Condens. Matter Phys.* **10**, 155 (2019).
- [68] E. V. Thuneberg, S. K. Yip, M. Fogelström, and J. A. Sauls, Models for Superfluid  $^3\text{He}$  in Aerogel, *Phys. Rev. Lett.* **80**, 2861 (1998).
- [69] P. Sharma and J. A. Sauls, Magnetic susceptibility of the Balian-Werthamer phase of  $^3\text{He}$  in aerogel, *J. Low Temp. Phys.* **125**, 115 (2001).
- [70] P. Sharma and J. Sauls, Thermal conductivity of superfluid  $^3\text{He}$  in aerogel, *Physica (Amsterdam)* **329-333B**, 313 (2003).
- [71] S. Higashitani, M. Miura, M. Yamamoto, and K. Nagai, Microscopic theory of sound propagation in the superfluid He 3–aerogel system, *Phys. Rev. B* **71**, 134508 (2005).
- [72] D. T. Sprague, T. M. Haard, J. B. Kycia, M. R. Rand, Y. Lee, P. J. Hamot, and W. P. Halperin, Effect of Magnetic Scattering on the  $^3\text{He}$  Superfluid State in Aerogel, *Phys. Rev. Lett.* **77**, 4568 (1996).
- [73] H. Choi, K. Yawata, T. M. Haard, J. P. Davis, G. Gervais, N. Mulders, P. Sharma, J. A. Sauls, and W. P. Halperin, Specific Heat of Disordered Superfluid  $^3\text{He}$ , *Phys. Rev. Lett.* **93**, 145301 (2004).
- [74] J. A. Sauls, Y. M. Bunkov, E. Collin, H. Godfrin, and P. Sharma, Magnetization and spin diffusion of liquid  $^3\text{He}$  in aerogel, *Phys. Rev. B* **72**, 024507 (2005).
- [75] S. N. Fisher, A. M. Guénault, N. Mulders, and G. R. Pickett, Thermal Conductivity of Liquid  $^3\text{He}$  in Aerogel: A Gapless Superfluid, *Phys. Rev. Lett.* **91**, 105303 (2003).
- [76] H. C. Choi, N. Masuhara, B. H. Moon, P. Bhupathi, M. W. Meisel, Y. Lee, N. Mulders, S. Higashitani, M. Miura, and K. Nagai, Ultrasound Attenuation of Superfluid  $^3\text{He}$  in Aerogel, *Phys. Rev. Lett.* **98**, 225301 (2007).
- [77] H. R. Ott, H. Rudigier, Z. Fisk, and J. L. Smith,  $\text{UBe}_{13}$ : An Unconventional Actinide Superconductor, *Phys. Rev. Lett.* **50**, 1595 (1983).
- [78] H. R. Ott, H. Rudigier, Z. Fisk, and J. L. Smith, Phase transition in the superconducting state of  $\text{U}_{1-x}\text{Th}_x\text{Be}_{13}$  ( $x = 0 - 0.06$ ), *Phys. Rev. B* **31**, 1651 (1985).
- [79] J. S. Kim, B. Andraka, and G. R. Stewart, Investigation of the second transition in  $\text{U}_{1-x}\text{Th}_x\text{Be}_{13}$ , *Phys. Rev. B* **44**, 6921 (1991).
- [80] B. Batlogg, D. Bishop, B. Golding, C. M. Varma, Z. Fisk, J. L. Smith, and H. R. Ott,  $\lambda$ -Shaped Ultrasound-Attenuation Peak in Superconducting  $(\text{U}, \text{Th})\text{Be}_{13}$ , *Phys. Rev. Lett.* **55**, 1319 (1985).
- [81] X.-L. Qi, T. L. Hughes, S. Raghu, and S.-C. Zhang, Time-Reversal-Invariant Topological Superconductors and Superfluids in Two and Three Dimensions, *Phys. Rev. Lett.* **102**, 187001 (2009).
- [82] J. Sauls, Surface states, edge currents, and the angular momentum of chiral p-wave superfluids, *Phys. Rev. B* **84**, 214509 (2011).